Published in final edited form as:
J Magn Reson Imaging. 2012 November ; 36(5): 1168–1178. doi:10.1002/jmri.23739.

Time-Resolved Dual-Station Calf-Foot 3D Bolus Chase MR Angiography with Fluoroscopic Tracking

Casey P. Johnson, PhD, **Eric A. Borisch, MS**, **James F. Glockner, MD, PhD**, **Phillip M. Young, MD**, and **Stephen J. Riederer, PhD**
MR Research Laboratory and Department of Radiology, Mayo Clinic, 200 First St SW, Rochester, MN 55905

Abstract

Purpose—To refine, adapt, and evaluate the technical aspects of fluoroscopic tracking for generating dual-station high-spatial-resolution MR angiograms of the calves and feet using a single injection of contrast material.

Materials and Methods—Nine subjects (seven healthy volunteers followed by two patients) were imaged using a two-station calf-foot 3D time-resolved bolus chase MRA protocol which provided <1.0 mm^3 spatial resolution throughout and 2.5 and 6.6 sec frame times at the calf and foot stations, respectively. Real-time reconstruction of calf station time frames allowed visually-guided triggering of table advance to the foot station. The studies were independently read and scored by two radiologists in six image quality categories.

Results—On average, overall diagnostic quality at the calf and foot stations was good-to-excellent, the calf arteries and all but the smallest foot arteries had good-to-excellent signal and sharpness, artifact and venous contamination were minor, and signal continuity across the inter-station interface was good.

Conclusion—The feasibility of fluoroscopic tracking has been demonstrated as an efficient approach for high spatiotemporal imaging of the arteries of the calves and feet with good-to-excellent diagnostic quality and low degrading venous contamination.

Keywords

contrast-enhanced MR angiography (CE-MRA); time-resolved; real-time; bolus chase; lower extremities; fluoroscopic tracking

INTRODUCTION

The arteries of the calves and feet are an important but challenging vascular region to image. In patients with peripheral arterial disease or diabetes mellitus, it is often desirable to image the arteries from the knees to the toes to diagnose vascular disease and to identify patent vessels for potential bypass grafts. Imaging of the peripheral vessels is complicated by their small size, the potential for rapid arterial-to-venous transit and complex and asymmetrical flow, and the need for extensive superior/inferior (S/I) coverage. Therefore, effective angiographic imaging of the calves and feet requires adequately high spatial resolution (~1.0 mm^3 for the calves, <1.0 mm^3 for the feet), precise timing to avoid venous contamination, and imaging over an extended FOV (>50 cm). 3D contrast-enhanced MR angiography (CE-

Corresponding Author: Stephen J. Riederer, PhD, 200 First St SW, Rochester, MN 55905, Tel: 507-284-6209, Fax: 507-284-9778, riederer@mayo.edu.

MRA) is used for lower extremity imaging and exploits such methods as single-station imaging using acceleration techniques, multi-station bolus chase MRA, and hybrid techniques. However, each of these methods has limitations.

Contemporary single-station time-resolved CE-MRA methods allow calf and foot angiograms to be acquired individually with high spatial resolution and frame times of 7 sec or less (1–6). Such methods can routinely avoid venous contamination and do not require an estimate of bolus transit time. However, due to the limited S/I coverage of a single station, typically ≤50 cm, two scans are generally necessary to image the arteries from the knees to the toes. This approach is inefficient, requiring multiple contrast-enhanced runs, possibly with a waiting period between runs to allow contrast clearance from the first injection.

Multi-station bolus chase MRA methods aim to image angiograms with extended S/I coverage (>50 cm) by advancing the scanner table to keep pace with the advancing contrast bolus (7–11). However, avoiding venous contamination at the calves and feet can be problematic, and often the feet are excluded in these exams or are imaged with relatively low spatial resolution. To image proximal stations with adequate spatial resolution generally requires an extended MR data acquisition time that results in the table advance lagging the advancing contrast bolus. Consequently, once the table is advanced to the distal-most station, the contrast transit may be well into or even past the arterial-only phase. To allow the table to reach the calves and feet in synchrony with the advancing contrast bolus, the imaging duration at each proximal station must be kept short, but this in turn limits spatial resolution. A further complication is that the patient-specific bolus transit time must often be estimated beforehand, such as with a timing bolus (12) and often at multiple locations (13,14).

Hybrid methods use a dual-contrast-injection approach to separately acquire a single-station time-resolved angiogram at the distal-most station in addition to a bolus chase extended FOV angiogram to better avoid venous contamination (15–22). The time-resolved acquisition is generally performed first and acts as a surrogate timing bolus for the bolus-chase run. To conserve contrast material, efforts have been made to reduce the contrast dose for the dynamic acquisition. However, the S/I coverage of this technique is typically insufficient to provide dynamic imaging from the knees to the toes.

Recently, a method called “fluoroscopic tracking” has been described (23) which attempts to combine the advantages of 3D time-resolved CE-MRA, bolus chase MRA, and real-time image reconstruction. At a proximal station, high-spatial-resolution images are acquired every few seconds and reconstructed in real time, allowing the operator to visually track the progressing contrast bolus and trigger table advance to a distal station. Such an approach can potentially allow efficient, dynamic, and extended FOV imaging of the lower extremities. Initial results were shown for dual-station thigh-calf imaging. The purpose of this work is to refine the fluoroscopic tracking technique and adapt it to high-spatial-resolution dual-station CE-MRA of the calves and feet and in so doing address the added challenges of smaller vessels and more dilute contrast material in this more distal region.

MATERIALS AND METHODS

Subjects

13 subjects comprised of 11 healthy volunteers (eight females, mean age 46, age range 31–58; three males, mean age 46, age range 33–63) followed by two patients (one female aged 67; one male aged 55) were consecutively enrolled for participation in an institutional review board-approved HIPAA-compliant prospective study. Each subject provided written informed consent. The first four studies were used to develop and refine the imaging

protocol. The latter nine studies, consisting of seven healthy volunteers (5 females, mean age 45, age range 31–54; 2 males aged 33 and 43) and the two patients, were used to evaluate the fluoroscopic tracking method using the refined protocol which is reported here.

Fluoroscopic Tracking Technical Specifications

"Fluoroscopic tracking" can be defined in multi-station CE-MRA as a technique in which 3D time-resolved images are formed of the vasculature of a station with: (i) adequate spatial resolution to allow diagnostic interpretation; (ii) adequate temporal resolution to allow visualization of bolus advance; and (iii) adequate reconstruction speed to allow the operator to interactively trigger table advance to the next station. As with fluoroscopic "triggering" (24,25), tracking requires that the temporal resolution be adequate for visualizing contrast bolus arrival and progression. However, more stringent than triggering, the spatial resolution of the tracking images must allow diagnostic interpretation, ideally as high-spatial-resolution 3D images.

For this work at the calf station we targeted: (i) ≤1.0 mm isotropic spatial resolution to be competitive with single-station CE-MRA techniques; (ii) ≤2.5 sec frame time to allow precise triggering of table motion based on typical times for contrast material to traverse the calf region (26); and (iii) <1.0 sec reconstruction latency for rapid triggering of table motion. To achieve a frame time this short with spatial resolution this fine, it is generally necessary to use view sharing (27), a method in which images are reconstructed at intervals shorter than the time necessary to acquire data for a single image with full spatial resolution, this latter time being defined as the temporal footprint (28). In the technical feasibility studies of Ref. (23), the temporal footprint was almost 20 sec long. When the transit time of the contrast bolus through the proximal station was shorter than this, which was not uncommon, the images in that station were thus incompletely sampled, resulting in loss of spatial resolution.

The above technical specifications of frame time and spatial resolution were achieved using the time-resolved Cartesian Acquisition with Projection Reconstruction-like sampling (CAPR) technique (28). To address the above-described issue of spatial resolution loss due to extended temporal footprint, the extent of sampling of the central k-space region was reduced for each frame and the degree of view sharing was reduced from eight to five vane sets compared to the method of Ref. (23). This allowed reduction of the temporal footprint from 19.1 to 12.1 sec with some minor loss of signal. Details are presented in recent work (29). Each fluoroscopic tracking image was reconstructed in <500 msec using a custom-built real-time system similar to that described in Ref. (23).

Because the foot station was the most distal station imaged, there was no need for the short frame time required for precise fluoroscopic tracking. Similarly, because the table was not being further advanced, the temporal footprint could be extended. Thus, larger values of frame time (6.6 sec) and temporal footprint (24.2 sec) were used for the foot vs. the calf station.

Imaging Protocol

All 13 subjects enrolled in this study were imaged using a 3T MRI system (Signa v14x; GE Healthcare; Waukesha, WI). The final nine subjects were imaged using the following protocol. Subjects were positioned feet-first in the scanner bore. The calves and feet were wrapped in warm blankets to minimize motion and promote arterial flow in the feet via vasodilation. Each subject was positioned with the soles of his/her feet pressed onto an angled plastic wedge to provide stability. Two custom-built receiver arrays, each with eight 27-cm-long coil elements, were used for imaging—one placed circumferentially around the

calves and the other similarly about the feet. All 16 coil elements were activated for the entire two-station imaging duration, which was found to improve signal coverage at the inter-station interface. For all studies 2D SENSE with acceleration R=8 was used at both stations.

The imaging protocol is shown in Figure 1. All subjects received a single dose of contrast material, 20 mL gadobenate dimeglumine (MultiHance; Bracco Diagnostics; Princeton, NJ) followed by 20 mL saline flush, administered via power injector (Spectris Solaris; Medrad Inc; Indianola, PN) at 3.0 mL/sec. The subjects' weights ranged from 56 to 103 kg (mean 78 kg), which yielded contrast doses ranging from 0.10 to 0.18 mmol/kg (mean 0.13 mmol/kg). Time-resolved 3D angiograms at the calves and feet were acquired using a fast spoiled GRE pulse sequence in a coronal format with frequency encoding superior/inferior (S/I), phase encoding left/right (L/R), and slice encoding anterior/posterior (A/P). Typical imaging parameters are shown in Table 1. Due to software limitations, it was necessary for some parameters such as TR, TE, and the number of frequency encoding samples to be fixed for both stations. Also, the S/I coverage of each station was limited to ≤35 cm due to the need to use a high performing gradient system to lower the TR while acquiring high spatial resolution data at the foot station. The total extended FOV was 62.5 cm with a triggered table advance of 30 cm in 5.5 sec. The table was triggered by the operator after the contrast bolus traversed the later-filling calf of each healthy volunteer and the target diseased calf of each patient. Rather than trigger immediately after contrast arrival at the distal calf FOV, triggering was delayed one or two frames to allow increased enhancement of the major distal calf arteries. After triggering, acquisition of the current frame was completed, followed by a command for table advance.

Image Quality Evaluation

Time series volumes and maximum intensity projections (MIPs) were reconstructed for radiological scoring of the seven healthy volunteer and two patient studies (n=9). Two radiologists (14 and 2 years of experience) independently read and scored each study in six categories (Table 2). Scores were assigned on a scale of 1 to 4, with general definitions being: 1, poor; 2, marginal; 3, good; and 4, excellent. Each leg was individually scored in all six categories. Categories I and II, arterial signal and arterial sharpness, were evaluated for each of 12 target arterial segments: popliteal; tibioperoneal trunk; proximal and distal anterior tibial; proximal and distal posterior tibial; proximal and distal peroneal; dorsalis pedis; lateral plantar; medial plantar; and planter arch. Additionally, it was noted whether portrayal of the digital arteries of each foot was of diagnostic quality. Categories III, IV, and V, presence of artifact, venous contamination, and overall diagnostic quality, were evaluated separately at both the calf and foot stations. Category VI, signal continuity across the calf-foot station interface, was evaluated considering the full extended FOV.

Bolus Arrival, Bolus Traversal, and Trigger Times

To assess contrast bolus dynamics at the calf station of each study, the times post-initiation of contrast injection at which the contrast bolus first arrived at and first completely traversed the calf station were determined for each leg from the tracking images. These times, referred to as the bolus arrival and traversal times, were determined by tracking the bolus leading edge, which has been shown in previous work to be sharply depicted by the CAPR technique (30). The calf station transit time was defined as the difference between the bolus traversal and arrival times. The triggering delay was defined as the difference between the trigger time and the bolus traversal time of the later-filling leg.

Statistical Analysis

The mean and standard error of the mean of the scores for each image quality evaluation category across the nine studies were calculated for each reader and in aggregate. The percentage of feet in which images of the digital arteries were of diagnostic quality was determined. Arterial segments deemed to not enhance due to disease were not included in the analysis. The mean, standard error of the mean, and range of the contrast bolus arrival, traversal, transit, table motion trigger, and trigger delay times at the calf station were also calculated.

CTA Comparison

The two patients recruited for this study were also imaged using a standard clinical runoff CTA exam on the same day as the CE-MRA exam, which provided a qualitative comparison of the peripheral vasculature. The CTA protocol used a 64-slice multi-detector imaging system (Definition; Siemens; Erlangen, Germany), which provided coverage from 4 cm above the iliac crest to the toes. Imaging parameters included 0.5 sec rotation time, 0.8 pitch, 15 mm/rotation, 120 kVp, 250 mA, and $0.6 \times 0.6 \times 2.0$ mm^3 spatial resolution. 145 mL of iodinated contrast material (Iohexol; Omnipaque 350; GE Healthcare; Waukesha, WI) was injected (25 mL at 5 mL/sec; 120 mL at 4 mL/sec) and followed by 30 mL of saline at 4 mL/sec. Automated triggering and exposure control were used. In accordance with standard clinical practice at our institution, the first run was immediately followed by a second to image from the knees to the toes in case the first run missed the bolus. For display, bones were manually segmented from the CT angiograms.

RESULTS

Fluoroscopic tracking was technically successful in all studies in that contrast arrival and traversal was observed in real time at the calf station and table motion was successfully triggered upon operator command. Tables 3 and 4 show scores for each image quality evaluation category. At the calf station, arterial signal and sharpness were generally rated excellent for proximal vessels and good-to-excellent for distal vessels, artifact was minor, venous contamination was non-present, and overall diagnostic quality was excellent. At the foot station, arterial signal and sharpness were generally scored excellent for the dorsalis pedis artery, good-to-excellent for the plantar arch, good for the lateral plantar artery, and marginal-to-good for the medial plantar artery. In aggregate, the only vessel segments to receive scores of poor signal and sharpness were 1/36 (2.8%) of both lateral plantar and plantar arch segments and 6/36 (16.7%) of medial plantar segments. The digital arteries were typically diagnostic. In spite of being the distal station, venous contamination and overall diagnostic quality at the foot station were typically scored minor and good, respectively.

Figure 2 shows a plot of the bolus arrival (circle), bolus traversal (square), and table motion triggering (triangle) times for both legs of all nine studies. For the patient studies, Subjects 8 and 9, the contrast bolus flow was asymmetrical in the two legs. Triggering was intentionally based on traversal in the later-filling leg for both cases, leading to delayed triggering and thus venous enhancement at the foot station in the earlier-filling leg. Averages and ranges for these times are shown in Table 5. Transit of the contrast bolus through the calf station took 7.5 sec (three times frames) on average, but ranged from 2.3 to 17.2 sec. Table motion was triggered on average 6.1 sec (two to three time frames) after the bolus leading edge traversed the later-filling leg.

Figures 3 and 4 show angiogram maximum intensity projections (MIPs) for a healthy volunteer, Subject 3. Time series MIPs of the individual calf and foot stations are shown in

Figures 3a and 3b, respectively. Figure 4 shows coronal and sagittal extended FOV MIPs created by combining the last calf and first foot time frames. A supplemental movie, Movie 1, shows the extended FOV time series.

Figure 5 shows results from the first patient, Subject 8, who had bilateral femoral-popliteal grafts. This study was performed because a more distal graft was being considered for the left leg, and triggering was thus based on contrast traversal in this leg. Images of the calf station (Figure 5a) show the delayed contrast arrival in the left vs. right leg and lack of signal in the left peroneal and posterior tibial arteries due to occlusion. The time series also shows distal perfusion and retrograde filling of the left posterior tibial artery (long arrow) via a communicating branch (short arrow). Sagittal images of the patient's left foot (Figure 5b) show a clear arterial phase time frame of the principal arteries. The temporal sharpness of the acquisition is illustrated in that only one frame (6.6 sec) later there is venous filling at the plantar arch. Supplemental movies are provided of the left calf and foot time series, Movies 2 and 3, respectively.

Figure 6 shows results from the second patient, Subject 9, who was imaged to assess discomfort in his distal right leg, and tracking was based on this side. The calf images (Figure 6a) show delayed filling of the right vs. left leg and near occlusion of the right anterior tibial artery. Triggering was performed based on transit of contrast material along the full extent of the right posterior tibial and peroneal arteries. Images of the patient's right foot (Figure 6b) show the arterial phase of the lateral and medial plantar and digital arteries but lack any simultaneous filling of the dorsalis pedis artery. Supplemental movies are provided of the right calf and foot time series in Movies 4 and 5, respectively.

Comparisons of CE-MRA and CTA angiogram targeted MIPs of the left calf of Subject 8 and the right calf of Subject 9 are shown in Figure 7. The CE-MRA and CTA MIPs show similar vascular morphology. In the feet, the close proximity of bones obscured the vessels in the CTA angiograms and the vessels were not as pronounced as in the calves, which prevented a qualitative comparison to the CE-MRA results.

DISCUSSION

3D time-resolved bolus chase MRA using real-time fluoroscopic tracking has been demonstrated for dual-station imaging of the arteries from the knees to the toes with sub-millimeter spatial resolution using a single injection of contrast material; i.e. with no test bolus. Despite use of high acceleration techniques, arterial signal and sharpness were scored as good-to-excellent in all but the smallest vessel segments. The diagnostic quality of small foot vessels such as the medial plantar and digital arteries is an indication of the high spatial resolution of the technique. Over the group of subjects studied, the fluoroscopic tracking technique enabled consistent imaging of both stations with good to excellent diagnostic quality.

An aspect of dual- or multi-station imaging that can be problematic is undesirable venous contamination at the distal station. In this work the average score across all studies for venous contamination for the foot station was 3.03; i.e. although there was some present, it was minor. Moderate venous contamination was typically only seen in the earlier-filling foot in situations of asymmetrical flow, which was the case in both patient studies. Owing to the high level of acceleration and the elliptical centric readout, the CAPR sequence can distinguish phenomena separated by as little as six seconds. An example of this is the patient study shown in Figure 5b and Movie 3. The first image, #18, acquired 49.8 sec after injection, portrays the arterial vasculature of the targeted foot. Because it was the first image formed at the foot station, the total acquisition time was one frame time, 6.6 sec. The next

image in the series, #19, 56.4 sec post-injection, has significant filling in the veins companion to the plantar arch. In spite of the rapid venous return in this region, the arteries are still clearly seen. It is acknowledged that this is but one example of intrinsic venous suppression, and additional patient studies are warranted.

Because it is a multi-station method, fluoroscopic tracking shares some of the limitations of standard, non-fluoroscopically-tracked bolus chase MRA. Specifically, in cases of asymmetrical flow, depending on when the table is moved either the later-filling calf may be imaged with an inadequately long acquisition time or the earlier-filling foot may have venous contamination. If only one leg is symptomatic, as was the case in the two patient studies reported here, then tracking can be based on this leg, and images of the other leg might not be relevant. However, if flow is markedly asymmetric and both legs need to be assessed, then fluoroscopic tracking could be followed with a targeted single-station acquisition using a second contrast injection if necessary.

A second limitation of multi-station CE-MRA applicable to fluoroscopic tracking is that due to the limited sampling time at a proximal station as a result of needing to advance the table, image quality within that station can be diminished, particularly for the later-filling distal vessels. This can be seen in the image quality evaluation in Table 3. Although the distal aspects of the three principal calf vessels had good-to-excellent arterial signal and sharpness, with mean aggregate scores in the 3.33 to 3.68 range, these scores were inferior to those of the proximal segments of the vessels. This can be seen another way. In Figure 3a note that proximal vessels are enhanced for five frames (#12 – #16), corresponding to a full 12.5 sec long temporal footprint and thus complete k-space coverage, while distal vessels are enhanced for only two or three frames (#14 – #16). As it is, even with the above constraint of a short (12.5 sec or less) net data acquisition time, the 1 mm isotropic spatial resolution is competitive with that of contemporary single-station methods for imaging the calf vessels; e.g. Refs. (4) and (21).

The demonstration of dual-station CE-MRA with fluoroscopic tracking provides motivation for other studies. The vast majority of imaging exams of the peripheral arteries in current clinical practice require coverage from the pelvis to the feet. Conceivably, the dual-station technique presented here could be extended to three or more stations, all with real-time tracking, while the calf and foot stations themselves could also be lengthened to extend the longitudinal coverage. In our own practice, CT angiography is often the firstline test for peripheral angiography. When this is inadequate distally, a focused calf-foot MRA exam as reported here can be useful. Another area of study is the contrast dose. Because the image acquisition times with tracking are short, it is likely that the contrast dose used in this study is greater than necessary. This is particularly true at the calf station, where the overall time spent for data acquisition, the sum of the “Bolus Transit” and “Triggering Delay” times in Table 5, can be as small as five frames (12.5 sec) or less. Ideally the bolus duration is no longer than the image acquisition time, as any excess duration represents contrast material which is not used. A reduction of the contrast dose, perhaps even as high 50%, would make additional contrast material available for imaging more proximal stations if desired. Yet another possible area of study is the use of real-time tracking with blood pool contrast agents. The first-pass arterial phase could be imaged at multiple stations with fluoroscopic tracking and followed with steady-state imaging for higher spatial resolution, but with the arteries having been identified from the first pass. Additionally, this would enable very rapid imaging of a pelvis and thigh station, while leaving sufficient time for a time-resolved dual-station calf-foot acquisition using the same contrast bolus.

This study had several limitations. First, the time to move the table from the calf to the foot station was 5.5 sec. Faster tables of the latest MRI systems allow this motion to occur within

about 3.0 sec, removing considerable dead time. Second, the receiver coil arrays used at each station were comprised of eight 27-cm-long coil elements. Increasing the coil count per array and the element length to, say, 40 cm would allow improved SENSE performance and extend the S/I coverage to 80 cm. Third, due to software limitations it was necessary to fix some scan parameters such as TR and TE to be the same for both stations. Allowing these to be station-specific would improve performance. Fourth, the number of subjects was limited, and more studies are necessary to assess overall reliability. However, even with this subject group the range of bolus arrival and transit times accommodated by fluoroscopic tracking was broad (Table 5). Lastly, direct comparison of the fluoroscopic tracking method to an established technique such as DSA is desirable to validate its diagnostic accuracy.

In conclusion, fluoroscopic tracking 3D bolus chase MRA has been demonstrated as an efficient technique for high spatiotemporal dual-station imaging of the arteries of the calves and feet using a single contrast injection.

Supplementary Material

Refer to Web version on PubMed Central for supplementary material.

Acknowledgments

The authors thank Kathy J. Brown for her assistance.

Funding: NIH grants EB000212, HL070620, and RR018898

REFERENCES

1. Ruhl KM, Katoh M, Langer S, et al. Time-resolved 3D MR angiography of the foot at 3 T in patients with peripheral arterial disease. AJR Am J Roentgenol. 2008; 190:W360–W364. [PubMed: 18492878]
2. Wu Y, Korosec FR, Mistretta CA, Wieben O. CE-MRA of the lower extremities using HYPR stack-of-stars. J Magn Reson Imaging. 2009; 29:917–923. [PubMed: 19306427]
3. Langer S, Kramer N, Mommertz G, et al. Unmasking pedal arteries in patients with critical ischemia using time-resolved contrast-enhanced 3D MRA. J Vasc Surg. 2009; 49:1196–1202. [PubMed: 19394548]
4. Haider CR, Glockner JF, Stanson AW, Riederer SJ. Peripheral vasculature: high-temporal- and high-spatial-resolution three-dimensional contrast-enhanced MR angiography. Radiology. 2009; 253:831–843. [PubMed: 19789238]
5. Lim RP, Jacob JS, Hecht EM, et al. Time-resolved lower extremity MRA with temporal interpolation and stochastic spiral trajectories: preliminary clinical experience. J Magn Reson Imaging. 2010; 31:663–672. [PubMed: 20187210]
6. Haider CR, Riederer SJ, Borisch EA, et al. High temporal and spatial resolution 3D time-resolved contrast-enhanced magnetic resonance angiography of the hands and feet. J Magn Reson Imaging. 2011; 34:2–12. [PubMed: 21698702]
7. Ho KY, Leiner T, de Haan MW, Kessels AG, Kitslaar PJ, van Engelshoven JM. Peripheral vascular tree stenoses: evaluation with moving-bed infusion-tracking MR angiography. Radiology. 1998; 206:683–692. [PubMed: 9494486]
8. Meaney JF, Ridgway JP, Chakraverty S, et al. Stepping-table gadolinium-enhanced digital subtraction MR angiography of the aorta and lower extremity arteries: preliminary experience. Radiology. 1999; 211:59–67. [PubMed: 10189454]
9. Nael K, Fenchel M, Krishnam M, Laub G, Finn JP, Ruehm SG. High-spatial-resolution whole-body MR angiography with high-acceleration parallel acquisition and 32-channel 3.0-T unit: initial experience. Radiology. 2007; 242:865–872. [PubMed: 17325071]

10. Vogt FM, Zenge MO, Ladd ME, et al. Peripheral vascular disease: comparison of continuous MR angiography and conventional MR angiography--pilot study. Radiology. 2007; 243:229–238. [PubMed: 17329687]
11. Maki JH, Wang M, Wilson GJ, Shutske MG, Leiner T. Highly accelerated first-pass contrast-enhanced magnetic resonance angiography of the peripheral vasculature: comparison of gadofosveset trisodium with gadopentetate dimeglumine contrast agents. J Magn Reson Imaging. 2009; 30:1085–1092. [PubMed: 19856442]
12. Earls JP, Rofsky NM, DeCorato DR, Krinsky GA, Weinreb JC. Breath-hold single-dose gadolinium-enhanced three-dimensional MR aortography: usefulness of a timing examination and MR power injector. Radiology. 1996; 201:705–710. [PubMed: 8939219]
13. Pereles FS, Collins JD, Carr JC, et al. Accuracy of stepping-table lower extremity MR angiography with dual-level bolus timing and separate calf acquisition: hybrid peripheral MR angiography. Radiology. 2006; 240:283–290. [PubMed: 16709792]
14. Potthast S, Wilson GJ, Wang MS, Maki JH. Peripheral moving-table contrast-enhanced magnetic resonance angiography (CE-MRA) using a prototype 18-channel peripheral vascular coil and scanning parameters optimized to the patient's individual hemodynamics. J Magn Reson Imaging. 2009; 29:1106–1115. [PubMed: 19388111]
15. Meissner OA, Rieger J, Weber C, et al. Critical limb ischemia: hybrid MR angiography compared with DSA. Radiology. 2005; 235:308–318. [PubMed: 15716387]
16. Janka R, Fellner C, Wenkel E, Lang W, Bautz W, Fellner FA. Contrast-enhanced MR angiography of peripheral arteries including pedal vessels at 1.0 T: feasibility study with dedicated peripheral angiography coil. Radiology. 2005; 235:319–326. [PubMed: 15731370]
17. Lapeyre M, Kobeiter H, Desgranges P, Rahmouni A, Becquemin JP, Luciani A. Assessment of critical limb ischemia in patients with diabetes: comparison of MR angiography and digital subtraction angiography. AJR Am J Roentgenol. 2005; 185:1641–1650. [PubMed: 16304027]
18. Tongdee R, Narra VR, McNeal G, et al. Hybrid peripheral 3D contrast-enhanced MR angiography of calf and foot vasculature. AJR Am J Roentgenol. 2006; 186:1746–1753. [PubMed: 16714669]
19. Andreisek G, Pfammatter T, Goepfert K, et al. Peripheral arteries in diabetic patients: standard bolus-chase and time-resolved MR angiography. Radiology. 2007; 242:610–620. [PubMed: 17179394]
20. Berg F, Bangard C, Bovenschulte H, et al. Hybrid contrast-enhanced MR angiography of pelvic and lower extremity vasculature at 3.0 T: initial experience. Eur J Radiol. 2009; 70:170–176. [PubMed: 18243622]
21. Attenberger UI, Haneder S, Morelli JN, Diehl SJ, Schoenberg SO, Michaely HJ. Peripheral arterial occlusive disease: evaluation of a high spatial and temporal resolution 3-T MR protocol with a low total dose of gadolinium versus conventional angiography. Radiology. 2010; 257:879–887. [PubMed: 20959539]
22. Floery D, Fellner FA, Fellner C, et al. Time-resolved contrast-enhanced MR angiography of the lower limbs: solving the problem of venous overlap. Rofo. 2011; 183:136–143. [PubMed: 20938886]
23. Johnson CP, Haider CR, Borisch EA, Glockner JF, Riederer SJ. Time-resolved bolus-chase MR angiography with real-time triggering of table motion. Magn Reson Med. 2010; 64:629–637. [PubMed: 20597121]
24. Wilman AH, Riederer SJ, King BF, Debbins JP, Rossman PJ, Ehman RL. Fluoroscopically triggered contrast-enhanced three-dimensional MR angiography with elliptical centric view order: application to the renal arteries. Radiology. 1997; 205:137–146. [PubMed: 9314975]
25. Riederer SJ, Bernstein MA, Breen JF, et al. Three-dimensional contrast-enhanced MR angiography with real-time fluoroscopic triggering: design specifications and technical reliability in 330 patient studies. Radiology. 2000; 215:584–593. [PubMed: 10796943]
26. Prince MR, Chabra SG, Watts R, et al. Contrast material travel times in patients undergoing peripheral MR angiography. Radiology. 2002; 224:55–61. [PubMed: 12091662]
27. Riederer SJ, Tasciyan T, Farzaneh F, Lee JN, Wright RC, Herfkens RJ. MR fluoroscopy: technical feasibility. Magn Reson Med. 1988; 8:1–15. [PubMed: 3173063]

28. Haider CR, Hu HH, Campeau NG, Huston J 3rd, Riederer SJ. 3D high temporal and spatial resolution contrast-enhanced MR angiography of the whole brain. Magn Reson Med. 2008; 60:749–760. [PubMed: 18727101]

29. Polley, TW.; Johnson, CP.; Riederer, SJ. Method for high spatial resolution of proximal stations in 3D time-resolved fluoroscopically-triggered bolus chase MRA. Proc 19th Annual Meeting ISMRM; May 7–13, 2011; Montreal, Quebec, Canada. p. 1295

30. Mostardi PM, Haider CR, Rossman PJ, Borisch EA, Riederer SJ. Controlled experimental study depicting moving objects in view-shared time-resolved 3D MRA. Magn Reson Med. 2009; 62:85–95. [PubMed: 19319897]

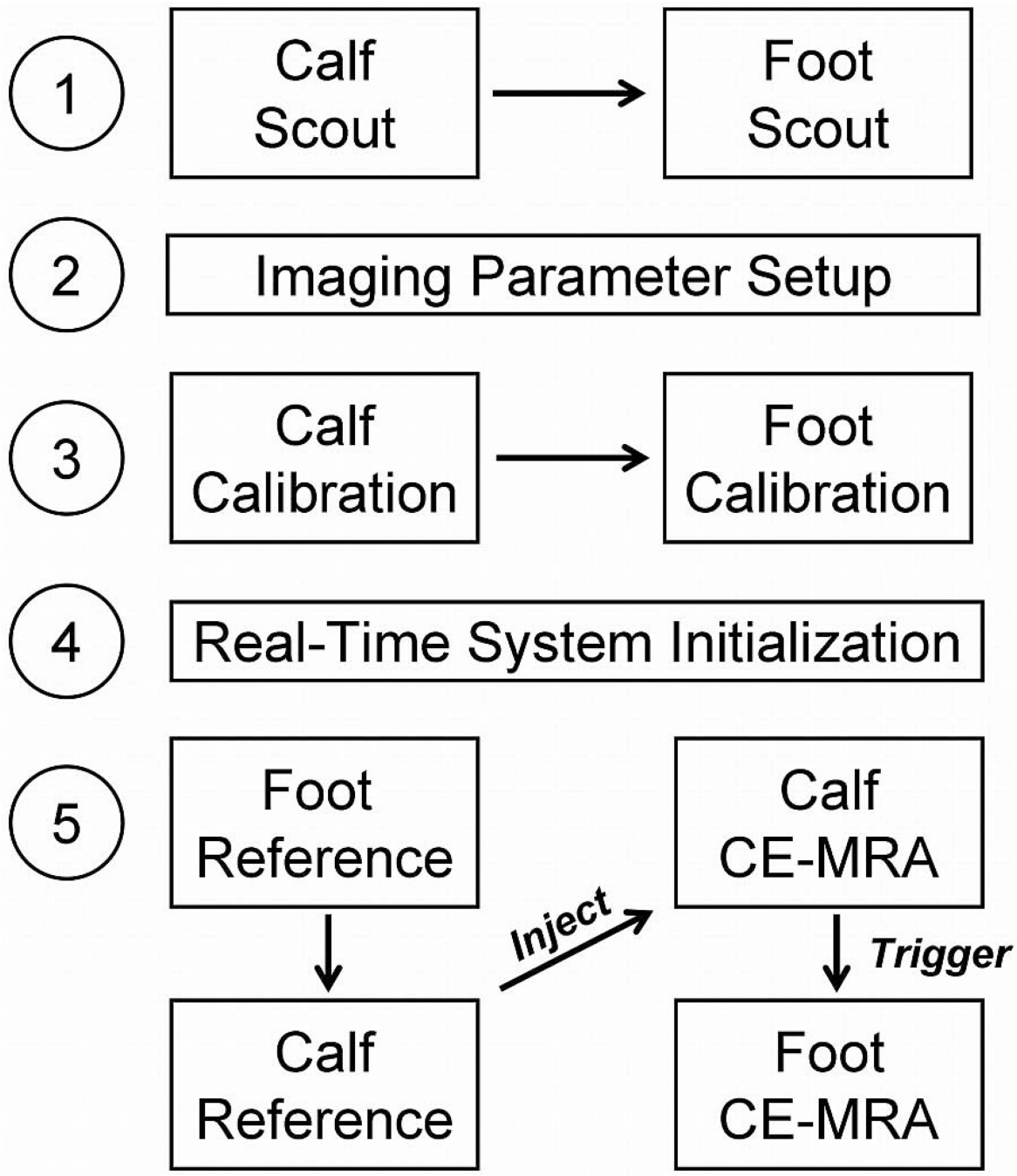

Figure 1.

Imaging protocol for 3D calf-foot fluoroscopic tracking. After scout images are acquired at both stations and imaging parameters are established for the remaining protocol steps, calibration images are acquired for 2D SENSE reconstruction. After initialization of the real-time system and calculation of SENSE inversion matrices, subtraction reference images and the time-resolved fluoroscopic tracking CE-MRA angiograms are all acquired seamlessly in real-time. Contrast material is injected immediately following acquisition of the reference images, and table advance from the calf to the foot station is triggered by the operator based on real-time visualization of the contrast bolus transit through the calf station.

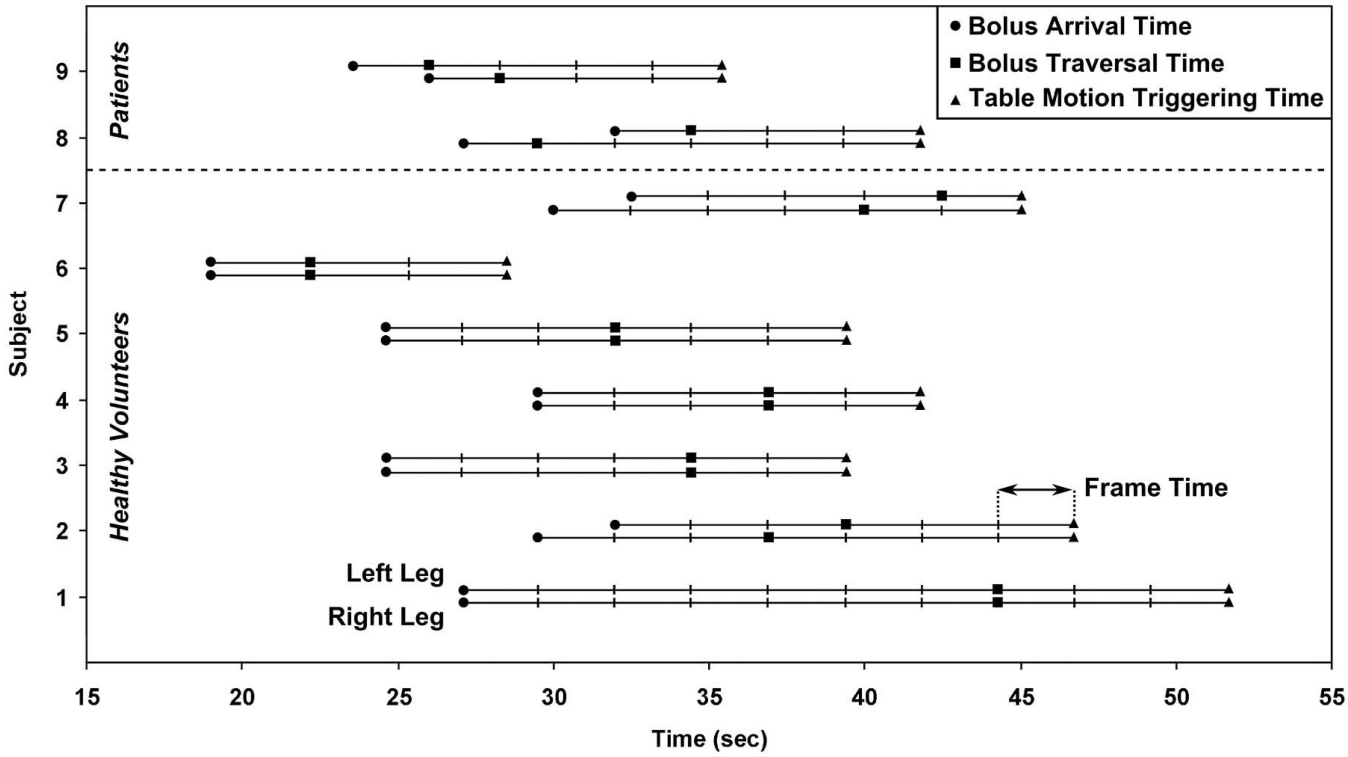

Figure 2.

Plot of contrast bolus arrival and traversal times and table motion triggering times at the calf station for all nine studies. Times are given relative to the initiation of contrast injection and are plotted for both the right and left legs. Hash marks indicate time frame intervals. Subjects 1–7 are healthy volunteers, and Subjects 8–9 are patients.

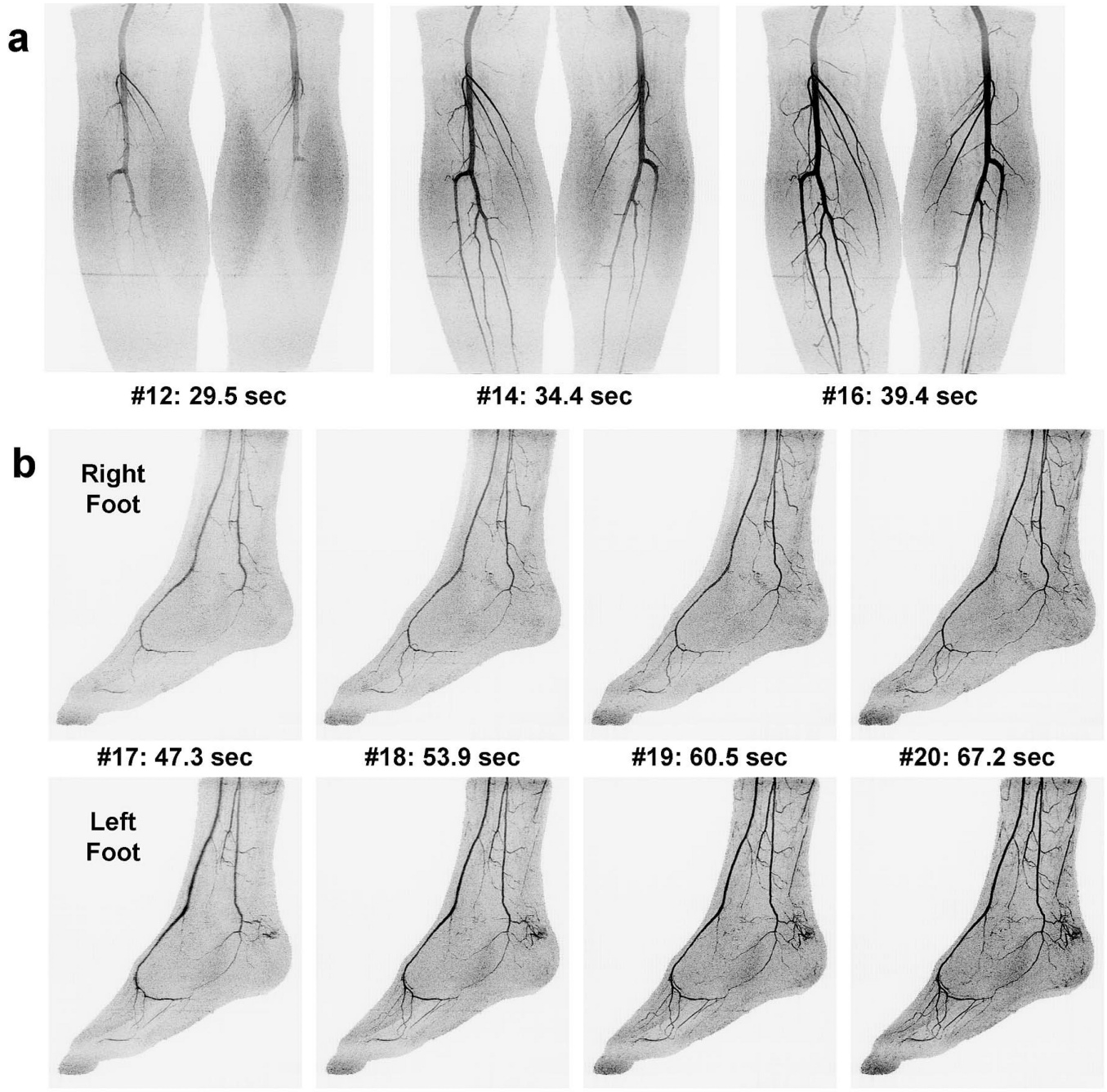

Figure 3.

Times series angiogram MIPs of a healthy volunteer study (Subject 3). **(a)** Coronal calf station time series showing the final calf frame (#16) and two preceding frames. The time and frame number post-contrast injection are indicated. Triggering of table motion occurred after viewing frame #15 (not shown). **(b)** First four foot station time frames shown separately for the right and left feet in a sagittal format. Only benign superficial venous contamination is seen in the early foot frames. See Movie 1 for additional detail.

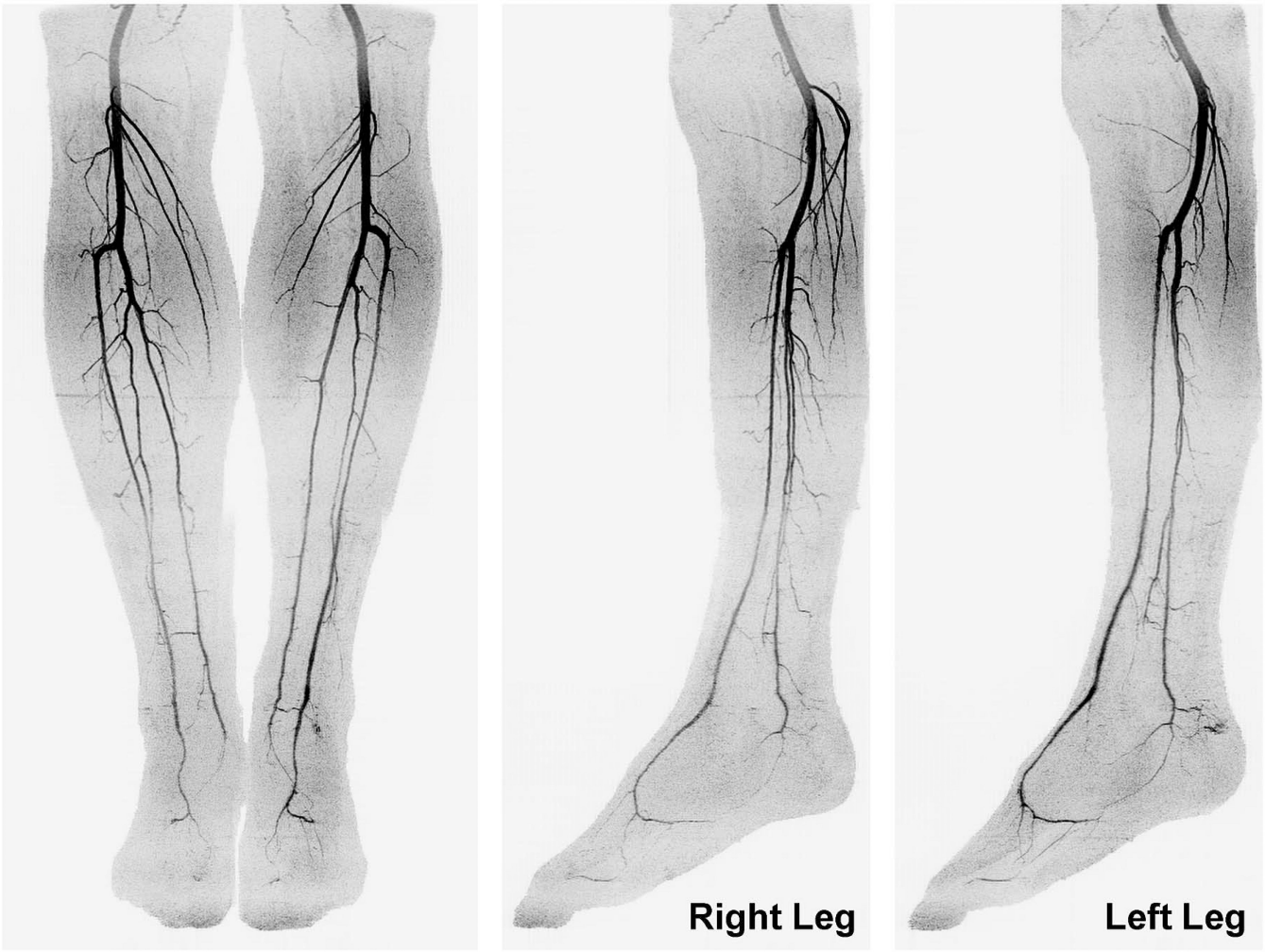

Figure 4.
Coronal and sagittal extended FOV MIPs for Subject 3 created by combining the last calf frame (#16) and the first foot frame (#17) in Figure 3. The MIPs show a nearly pure arterial phase throughout the long FOV with sub-millimeter 3D resolution. Sagittal MIPs are shown separately for the right and left legs. See Movie 1 for additional detail.

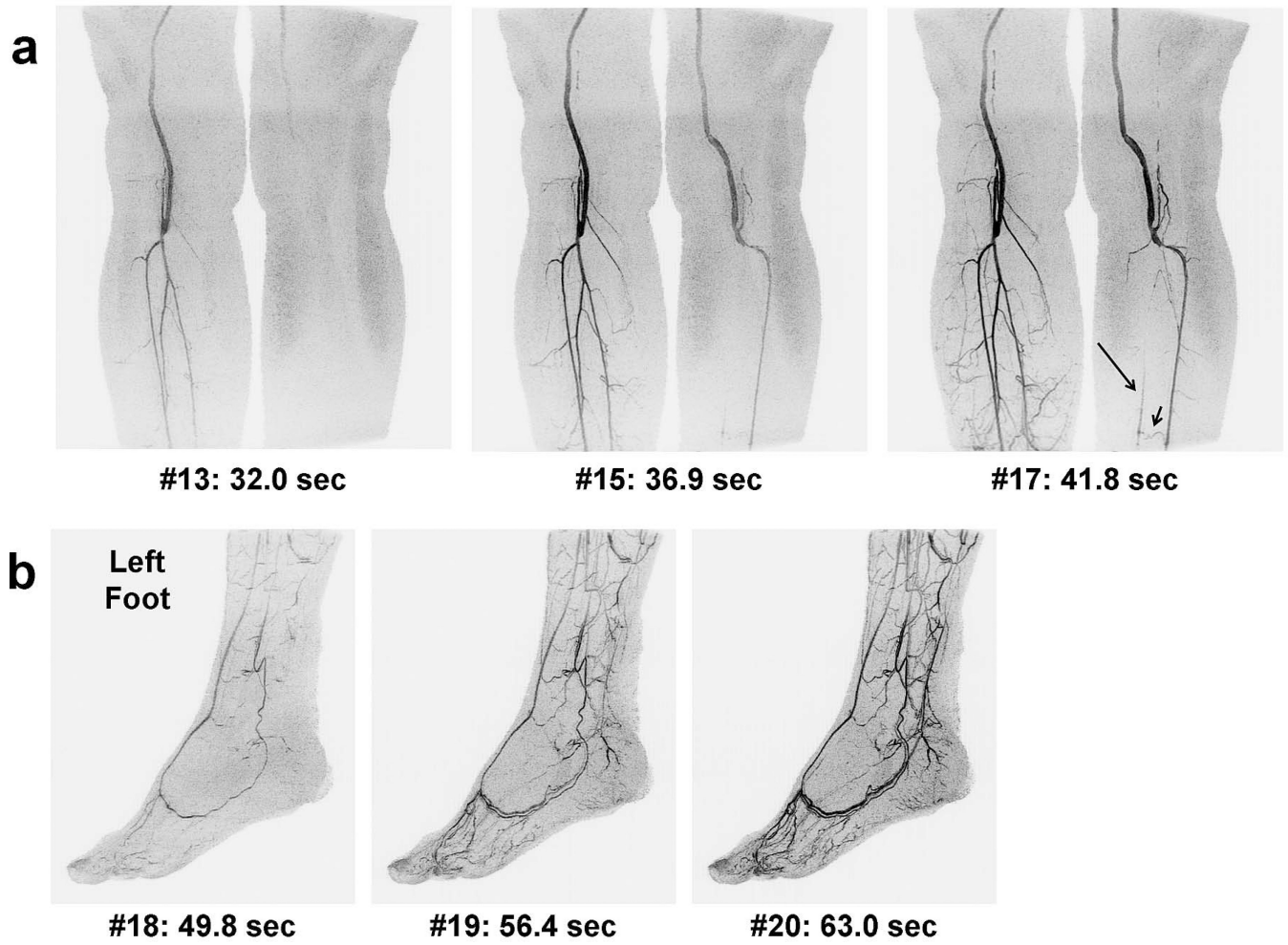

Figure 5.

Time series MIPs of the first patient study (Subject 8) shown in coronal format for the calves **(a)** and sagittal format for the left foot **(b)** with similar labels as in Figure 3. Tracking was based on bolus flow in the left leg due to interest in placing a distal graft. Note that the bolus traversed the right leg more rapidly than the left (29.5 vs. 34.4 sec), leading to venous enhancement in the right foot (not shown). The first frame (#18) of the left foot shows a mostly arterial phase. Venous enhancement rapidly progresses in subsequent frames. Disease is apparent in the left calf: the posterior tibial and peroneal arteries lack signal due to occlusion of the tibioperoneal trunk. The time-resolved nature of the exam allows visualization of retrograde filling of the posterior tibial artery (long arrow) via a communicating artery (short arrow). See Movies 2 and 3 for additional detail.

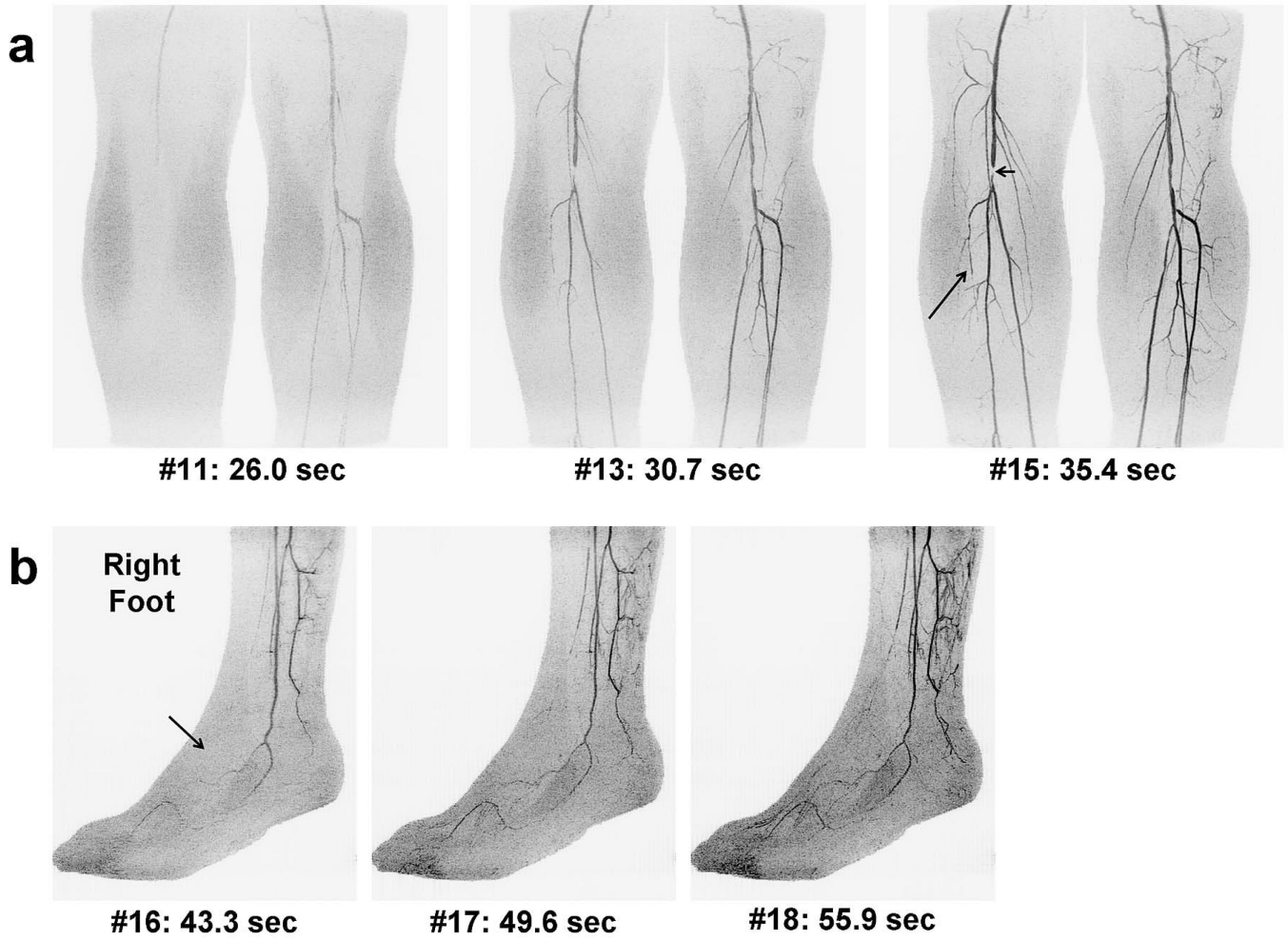

Figure 6.

Time series MIPs for the second patient study (Subject 9) with similar format as those in Figure 5. The right foot is shown in **(b)**. In this case, tracking was based on bolus transit through the right calf due to suspected disease on this side. As with Subject 8, bolus transit in the two legs was asymmetrical. The bolus traversed the left leg first (26.0 vs. 28.3 sec), leading to early venous enhancement of the left foot. The right calf shows occlusion of the anterior tibial artery (**a**, long arrow), contributing to lack of perfusion of the right dorsalis pedis artery (**b**, arrow). Stents had previously been placed in the right femoral artery, one of which caused localized signal loss (**a**, short arrow). See Movies 4 and 5 for additional detail.

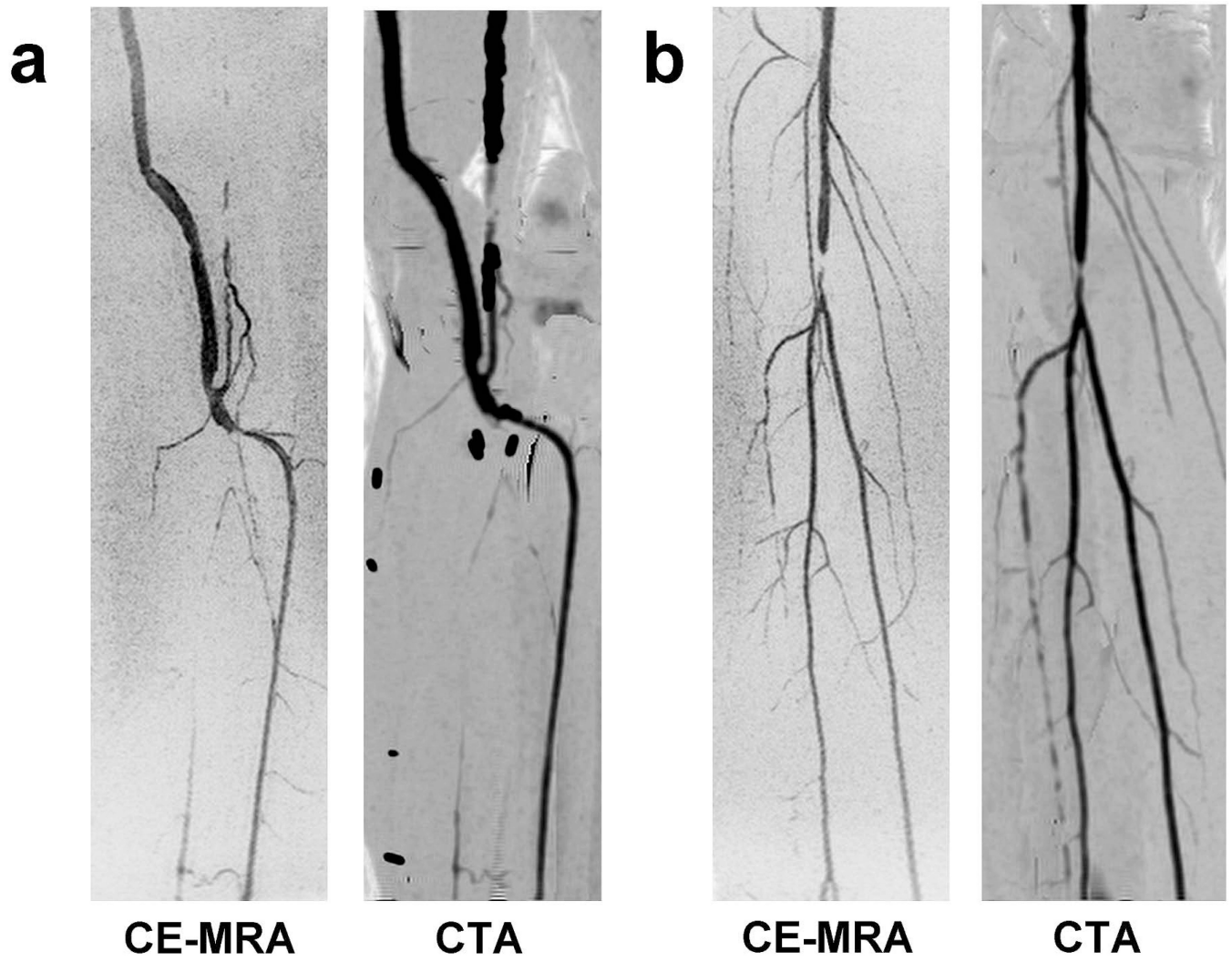

Figure 7.
Comparison of CE-MRA and CTA coronal targeted MIPs for the two patient studies: (**a**) Subject 8 and (**b**) Subject 9. The targeted MIPs are of the left calf for Subject 8 (see Figure 5) and the right calf for Subject 9 (see Figure 6). The CE-MRA MIPs were generated using the final time frame at the calf station. The vascular morphology and regions of disease match well between the two modalities.

Table 1

Typical imaging parameters used for the *in vivo* calf-foot CE-MRA studies. In a few cases, frame times varied slightly due to modification of the axial FOV or flip angle.

	Calf Station	Foot Station
FOV (cm: S/I × L/R × A/P)	35 × 31.2 × 13.2	30 × 19.8 × 24
Sampling Matrix (S/I × L/R × A/P)	400 × 312 × 132	400 × 264 × 256
Resolution (mm: S/I × L/R × A/P)	0.88 × 1.0 × 1.0	0.75 × 0.75 × 0.94
Flip Angle (°)	30	30
Bandwidth (kHz)	±62.5	±62.5
TR / TE (ms)	5.7 / 2.6	5.7 / 2.6
2D SENSE Acceleration (L/R × A/P)	4 × 2	2 × 4
2D Partial Fourier Acceleration	1.98	1.88
Frame Time (sec)	2.5	6.6
Temporal Footprint (sec)	12.1	24.2

Table 2

Image quality evaluation categories and scoring.

Score	Category
	I. Arterial Signal – Target Vessels
1	Poor: insufficient signal for diagnosis
2	Marginal: low arterial signal but diagnosis can still be made
3	Good: minor arterial signal loss that does not interfere with diagnosis
4	Excellent: arteries have high signal and are clearly distinguished from the background
	II. Arterial Sharpness – Target Vessels
1	Poor: blurring of arteries does not allow sufficient spatial resolution for diagnosis
2	Marginal: arteries blurred but spatial resolution still sufficient for diagnosis
3	Good: minor blurring of arteries does not interfere with diagnosis
4	Excellent: arteries imaged sharply with good spatial resolution
	III. Presence of Artifact – Calf and Foot Stations
1	Severe: non-diagnostic result
2	Moderate: interferes with diagnosis
3	Minor: does not interfere with diagnosis
4	No artifact
	IV. Venous Contamination – Calf and Foot Stations
1	Severe: non-diagnostic result
2	Moderate: interferes with diagnosis
3	Minor: does not interfere with diagnosis
4	No venous contamination
	V. Overall Diagnostic Quality – Calf and Foot Stations
1	Poor: non-diagnostic
2	Marginal: arteries blurred, have weak signal, or obscured but diagnosis can still be made
3	Good: arteries generally sharp with high signal and some minor obscureness or loss of quality
4	Excellent: arteries sharp with high signal and no obscureness
	VI. Signal Continuity Across Calf-Foot Station Interface – Extended FOV
1	Poor: signal discontinuous
2	Marginal: signal continuous with significant signal loss
3	Good: signal continuous with minor signal loss
4	Excellent: signal continuous with no signal loss

Table 3

Scores for image quality evaluation categories I and II (Nine subjects, right and left sides, and two readers yield an aggregate n=36).

Arterial Segment	Category I: Arterial Signal			Category II: Arterial Sharpness		
	Reader 1	Reader 2	Aggregate	Reader 1	Reader 2	Aggregate
Popliteal	4.00 ± 0.00	3.67 ± 0.11	3.83 ± 0.06	4.00 ± 0.00	3.78 ± 0.10	3.89 ± 0.05
Tibioperoneal Trunk	4.00 ± 0.00	4.00 ± 0.00	4.00 ± 0.00	4.00 ± 0.00	4.00 ± 0.00	4.00 ± 0.00
Proximal Anterior Tibial	3.94 ± 0.06	4.00 ± 0.00	3.97 ± 0.03	3.94 ± 0.06	4.00 ± 0.00	3.97 ± 0.03
Proximal Posterior Tibial	3.83 ± 0.12	4.00 ± 0.00	3.91 ± 0.06	3.89 ± 0.08	4.00 ± 0.00	3.94 ± 0.04
Proximal Peroneal	3.94 ± 0.06	3.89 ± 0.11	3.92 ± 0.06	3.94 ± 0.06	3.89 ± 0.11	3.92 ± 0.06
Distal Anterior Tibial	3.82 ± 0.10	3.35 ± 0.19	3.59 ± 0.11	3.71 ± 0.11	3.65 ± 0.15	3.68 ± 0.09
Distal Posterior Tibial	3.61 ± 0.12	3.22 ± 0.19	3.42 ± 0.12	3.39 ± 0.12	3.50 ± 0.17	3.44 ± 0.10
Distal Peroneal	3.44 ± 0.12	3.22 ± 0.19	3.33 ± 0.11	3.28 ± 0.11	3.50 ± 0.17	3.39 ± 0.10
Dorsalis Pedis	3.94 ± 0.06	3.82 ± 0.13	3.88 ± 0.07	3.75 ± 0.14	3.71 ± 0.19	3.73 ± 0.12
Lateral Plantar	3.00 ± 0.16	2.89 ± 0.23	2.94 ± 0.14	2.94 ± 0.17	2.61 ± 0.22	2.78 ± 0.14
Medial Plantar	2.50 ± 0.12	1.89 ± 0.18	2.19 ± 0.12	2.67 ± 0.11	1.67 ± 0.11	2.17 ± 0.12
Plantar Arch	3.33 ± 0.20	3.33 ± 0.23	3.33 ± 0.15	3.28 ± 0.19	3.28 ± 0.23	3.28 ± 0.15
Digital	78% (14/18)	67% (12/18)	72% (26/36)	-	-	-

With the exception of the digital arteries, all values are reported as mean ± standard error of the mean. The percentage of feet in which the digital arteries were of diagnostic quality is reported.

Table 4

Scores for image quality evaluation categories III, IV, V, and VI (readers: n=18; aggregate: n=36).

	Category III: Presence of Artifact		Category IV: Venous Contamination		Category V: Diagnostic Quality		Category VI: Signal Continuity
	Calf Station	Foot Station	Calf Station	Foot Station	Calf Station	Foot Station	Extended FOV
Reader 1	3.00 ± 0.00	3.00 ± 0.00	3.94 ± 0.06	2.83 ± 0.09	3.89 ± 0.08	2.89 ± 0.08	3.28 ± 0.16
Reader 2	3.22 ± 0.10	3.00 ± 0.00	4.00 ± 0.00	3.22 ± 0.22	3.89 ± 0.08	3.00 ± 0.11	3.22 ± 0.10
Aggregate	3.11 ± 0.05	3.00 ± 0.00	3.97 ± 0.03	3.03 ± 0.12	3.89 ± 0.05	2.94 ± 0.07	3.25 ± 0.09

All values are reported as mean ± standard error of the mean.

Table 5

Contrast bolus arrival, traversal, and transit times and table motion triggering and delay times at the calf station (bolus arrival, traversal, and transit times: n=18; triggering and delay times: n=9).

	Mean Time (sec)	Range (sec; min-max)
Bolus Arrival	26.8 ± 0.9	19.0 – 32.5
Bolus Traversal	34.3 ± 1.6	22.2 – 44.3
Bolus Transit	7.5 ± 1.1	2.3 – 17.2
Triggering of Table Motion	41.1 ± 2.2	28.5 – 51.7
Triggering Delay	6.1 ± 0.6	2.5 – 7.4

Mean times are reported as mean ± standard error of the mean.